Design earthquakes' map: an additional tool for engineering seismic risk analysis. Application to southern Apennines (Italy).

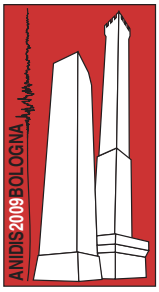

Vincenzo Convertito
Istituto Nazionale di Geofisica e Vulcanologia, Osservatorio Vesuviano. Via Diocleziano 328, 80124 Napoli.

Iunio Iervolino
Dipartimento di Ingegneria Strutturale, Università di Napoli Federico II. Via Claudio 21, 80125, Napoli.

Andrè Herrero
Istituto Nazionale di Geofisica e Vulcanologia. Via di Vigna Murata 605, 00143 Roma.

Keywords: seismic hazard, disaggregation, design earthquake.

ABSTRACT
Probabilistic seismic hazard analysis (PSHA) is currently the soundest basis for the evaluation of the hazard for site-specific engineering design purposes. An increasing number of building codes worldwide acknowledges the uniform hazard spectra as the reference ground motion to determine design actions on structures and to select input signals for seismic structural analysis. The new Italian seismic code requires the seismic input for nonlinear dynamic analysis to be selected on the basis of *dominating events*, e.g., identified via disaggregation of seismic hazard. In the present study, the design earthquakes expressed in terms of magnitude (*M*), distance (*R)* and ε, were investigated for a wide region in the southern Apennines, Italy. The hazards corresponding to peak ground acceleration and spectral acceleration at 1 second having 475-year return period were disaggregated. For each of the disaggregation variables the shapes of the joint and marginal probability density functions were studied and the first two modes of *M, R* and ε were extracted and mapped. The obtained results can be used as additional information to better identify the design earthquakes. Moreover, for the study area, they allow the assessment of the seismic source contribution to various frequency ranges of the design spectrum.

1 INTRODUCTION

From an engineering point of view, the most accurate analysis to assess the safety level of existing civil and/or strategic structures such as nuclear power plants, hospitals, bridges or lifelines in an earthquake prone-zone, implies nonlinear dynamic analysis. It allows to account for a large number of features of the ground shaking as, for example, peculiar spectral shape, cumulative damage potential (e.g., duration), nonstationarity and special effects, directivity-related velocity pulses (e.g., Iervolino and Cornell, 2008). As a consequence, it requires both detailed modelling of the structure and proper selection of the seismic ground motion input. The latter is typically comprised of a suite of time series "representative" of ground shaking that the structure must withstand during its life-time, based on the hazard at the site where the structure is located. The selection of recorded time histories from a given database, or their simulation through ad-hoc techniques, may require that an earthquake, defined as the "design earthquake", is prudently identified (Iervolino and Cornell, 2005). When the selection of recorded time histories for seismic design of structures is concerned, the current state of best engineering practice (e.g., U.S. Nuclear Regulatory Commission, 2001) is based on the uniform hazard spectrum (UHS) derived from the probabilistic seismic hazard (PSHA) at the site. The UHS is defined with the purpose that all its spectral ordinates have the same probability of exceedance in a time interval depending on the limit-state of interest. Once the UHS has been defined, for the level of spectral acceleration given by the UHS at the first oscillation period of the structure, the time histories' selection proceeds with the disaggregation of seismic hazard (e.g., McGuire, 1995), by magnitude (M), distance (R), and ε. The latter variable is defined as the number of logarithmic standard deviations by which the logarithmic ground motion departs from the median predicted by an appropriate attenuation relationship. Disaggregation is based on the computation of the relative contributions of the elements used to compute seismic hazard,

e.g., seismogenic zones, recurrence relationships, and as recently investigated, focal mechanisms (Convertito and Herrero, 2004). In particular, it allows the identification of the earthquakes which dominate the hazard as a function of the structural oscillation period, location, and return period. Those contributions are typically expressed in terms of probability density functions (PDFs) of M, R and ε conditional on the exceedance of the level of spectral acceleration, Sa(T), for which the hazard is disaggregated. The analysis of these PDFs, allows the identification of the design earthquake.

Given the dominant M, R, and ε values, along with other earthquake-specific characteristics, such as directivity, faulting style and duration, time histories can be selected for engineering analyses. In fact, after the design earthquake is identified, a database is accessed and a number of time histories is selected to match, within tolerable limits, the values of these parameters believed to be important for a correct estimation of the structural response.

Finally, the selected time histories are scaled to match precisely the UHS level at the first period (T) of the structure. Time histories obtained in this way are used as the input for a set of nonlinear dynamic analyses to evaluate the behaviour of the structure in the case of the ground motion represented by the UHS (Cornell, 2004).

Generally, prescriptions for time histories selection in building codes (e.g., Eurocode 8 – CEN, 2003) only approximate the approach discussed above (Iervolino et al., 2008). In fact, the code-based spectra may be very weakly related to the hazard and therefore may be quite different from the UHSs. In these cases disaggregation may still be useful to identify the controlling earthquake sources, but to relate the design spectra to the hazard requires the PSHA to be available for any site in the region where the code applies. This is not the case for many countries where engineers are seldom able to easily run or obtain hazard analyses for the site of interest. A fortunate case in this respect are the U.S., where hazard data may be downloaded by the U.S. Geological Survey (USGS) website. Italy also now has a similar service due to the work of the Istituto Nazionale di Geofisica e Vulcanologia (INGV) carried out in the framework of a specific project commissioned, between 2004 and 2006, by the Italian Civil Protection – *Dipartimento della Protezione Civile* (DPC). The results of the project include hazard curves on rock, based on 9 return periods, for 11 oscillation periods of engineering interest and disaggregation for the whole Italian territory (Meletti and Montaldo, 2007; Montaldo and Meletti, 2007). This study has been acknowledged by the new Italian seismic code (CS. LL. PP., 2008) which now allows to design considering response spectra derived from seismic hazard (technically coincident with the UHSs) and to select time histories with respect to the characteristics of the dominating earthquake.

The present study, based on similar premises of what was proposed by Cramer and Petersen (1996) for southern California, and Harmsen and Frankel (2001) for the U.S., investigates the implications of mapping the design earthquakes for spectral accelerations corresponding to different spectral frequency ranges via an application to the Campania-Lucania region in southern Apennines (Italy). In fact, the data made publicly available for Italy by INGV include disaggregation for peak ground acceleration (PGA) only (Spallarossa and Barani, 2007); however, short and long period ranges of the UHS may be affected by different seismic sources in terms of magnitude and distance (Reiter, 1990). This is important because design of moderate-to-long period structures has to consider dominant events which may be not well identified by the results of PGA hazard disaggregation.

For the study area, the maps of the first two modal magnitudes, distances and epsilons sets were computed from disaggregation of seismic hazard on rock sites, specifically calculated, for two spectral ordinates, PGA and Sa(T=1sec). The selected hazard level corresponds to 10% of probability of exceedance in 50 years, which is a reference return period for the life-safety limit-state of ordinary constructions. These maps may be tools to better identify the dominating earthquakes for each site (Bommer, 2004), and to assess how frequencies of the design spectrum of engineering interest are differently contributed by seismogenic sources in the area.

2 METHODOLOGY

The result of PSHAs, for a selected site, is a hazard curve that represents the probability of exceedance of a strong ground motion parameter A in a time interval of interest (e.g., the design life of a structure). The computation of the hazard curve, requires the solution of the hazard integral (Cornell, 1968; Bazzurro and Cornell, 1999) that,

for the *i*-th selected seismogenic zone and a range of possible magnitudes and distances, is given by:

$$E_i\left(A > A_o\right) = \\ = \alpha_i \int_M \int_R \int_\varepsilon I\left[A > A_o \left| m, r, \varepsilon \right.\right] f(m) f(r) \, dm \, dr \, d\varepsilon \quad (1)$$

where *I* is an indicator function that equals 1 if *A* is larger than A_o for a given distance *r*, ranging between R_{min} and R_{max}, a given magnitude *m*, ranging between M_{min} and M_{max}, and a given ε, which represents the residual variability of the *A* parameter with respect to the selected attenuation relationship. The PDFs of *M*, *f(m),* and *R*, *f(r)*, depend, respectively, upon the adopted earthquake recurrence model and upon the source geometry that can be a point, a line, a plane or an areal source zone. Finally, α_i for each zone, represents the mean annual rate of occurrence of the earthquakes within the source.

Assuming a Poissonian earthquake recurrence model, which is traditional in most PSHAs, Equation (1) allows the computation of the probability of exceedance *P* in a time interval *t* as in Equation (2), where the sum is over all the sources contributing to the hazard.

$$P\left(A > A_0, t\right) = 1 - e^{-\sum_{i=1}^{N} E_i\left(A > A_0\right) \cdot t} \quad (2)$$

PSHA, for its integral nature, combines the contributions to the hazard of all *N* considered sources. On the other hand, for engineering purposes it may be important to identify the most threatening earthquakes for the site of interest. The procedure that allows the decomposition of each point on the hazard curve, in terms of *M* and *R*, from each different source is the *disaggregation* (Bazzurro and Cornell, 1999). In the last decade, it has become common practice to also look at the disaggregation of seismic hazard in terms of ε. Given magnitude and distance, ε represents, via its associated PDF *f(ε)*, the variability of the ground motion parameter for which the hazard is estimated. Disaggregation in terms of ε may be useful so that one can choose records for nonlinear dynamic analysis having the *correct* spectral shape at a period relevant for the dynamic behavior of the structure.

From an analytical point of view, the disaggregation's result is the joint PDF in Equation (3), which is the distribution of magnitude, distance and ε conditional on the exceedance of the hazard level being disaggregated. In other words, given the exceedance of the A_0 ground motion value, disaggregation gives how likely it is caused by each specific *M*, *R*, ε set (McGuire, 1995).

$$f\left(m, r, \varepsilon\right) = \\ = \frac{\sum_{i=1}^{N} \alpha_i I\left[A > A_o \left| m, r, \varepsilon \right.\right] f(m) f(r) f(\varepsilon)}{\sum_{i=1}^{N} E_i\left(A > A_0\right)} \quad (3)$$

From the PDF in Equation (3) marginal PDFs may be obtained for M, R and ε alone, or for any pair comprised of two of them.

In the case one wants, or it is allowed by the seismic code, to use disaggregation of seismic hazard to identify the design earthquakes for the site of interest semi-arbitrary approaches based on these PDFs are usually adopted. For example, representative values of the distributions (modal or the mean values of *M*, *R*, and ε) may be considered if a single design earthquake is sought. The first step in the analyses proposed in the present study consisted in the computation of the hazard maps for the region shown in Figure 1 in terms of PGA and Sa(T=1sec).

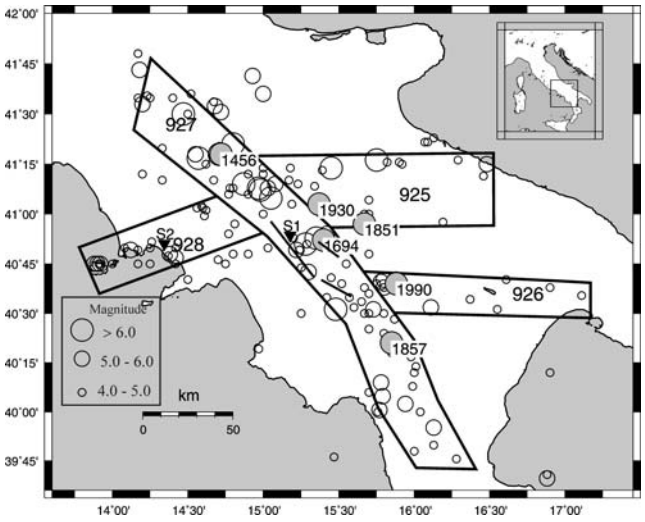

Figure 1: Seismic source zone configuration used to compute the hazard and design earthquakes maps. Location of the sites S1 and S2 used in the analysis is identified by inverted black triangles. Circles, whose width is proportional to magnitude, represent the location of the earthquakes (M > 4.0) retrieved from the CPTI04 catalogue (Gruppo di lavoro CPTI, 2004). Labels report the dates of some historical earthquakes. Black lines represent the surface projection of the three fault segments which ruptured during the 23 November 1980 Irpinia earthquake.

The choice of these two spectral ordinates is to represent the high and moderate-to-low frequency branches of the response spectrum respectively. This is important because, although this is known since some time, often both seismologists and engineers focus on hazard in terms of PGA only; on the other hand, seismic structural response is more sensitive to the spectral ordinates corresponding to lower frequencies. Therefore, the hazard should be better expressed in terms of spectral ordinates close to the fundamental period of the structure for which the seismic design or assessment is carried out. In fact, because disaggregation results, apart from the return period, also depend on such ordinate, it is worthwhile a comparison of the design earthquakes resulting from disaggregation of PGA and other spectral ordinates.

3 PROBABILISTIC SEISMC HAZARD ANALYSIS FOR SOUTHERN APENNINES

The southern Apennines is an active seismogenic belt consisting of different faults which were the site of historical (e.g., 1456, 1694, 1851, 1857, and 1930) and recent moderate seismicity (e.g., 5 May 1990 Potenza Mw 5.8). The last destructive earthquake occurring in the area of interest was the complex Irpinia earthquake (23 November 1980, Mw 6.9) which caused about 3,000 deaths and enormous damage (Westaway and Jackson, 1987). Most of the instrumentally recorded earthquakes have occurred in a narrow band along the Apennine chain (corresponding to zone 927 in Figure 1) in the top 20 km of the crust and reveals a prevailing extensional regime (Montone *et al.*, 2004) as indicated by normal faulting mechanisms (Valensise *et al.*, 2003).

Concerning the hazard elements, the modeling of the seismogenic zones in the southern Apennines region is that of the Italian zonation (ZS9) also adopted by the INGV (Meletti *et al.*, 2008), along with the activity rates, *b*-values, and minimum and maximum magnitudes that are listed in the Table 1.

Table 1. Table caption Parameters of the selected seismogenic zones shown in Figure 1.

Zone	α (events/year)	b	M_{min}	M_{max}
925	0.17	-0.75	4.0	6.83
926	0.09	-1.38	4.0	6.14
927	0.69	-0.72	4.0	7.06
928	0.21	-0.66	4.0	5.91

Figure 1 shows the location and the dates of the historical earthquakes cited above. Moreover, seismic events with magnitude larger than *M* 4.0, contained in the CPTI04 catalogue provided by the Gruppo di lavoro CPTI (2004) and used by INGV to compute the national hazard map, are also shown. Finally, same figure reports the three fault segments on which the 23 November 1980 Mw 6.9 Irpinia earthquake originated. The activity rates and the values selected for the analyses performed in this work are based on the historical catalogue adjusted for completeness. The historical catalogue also contains the main instrumental recorded earthquakes that occurred in the study area. The selected attenuation relationship considered is that of Sabetta and Pugliese (1996) which is derived from Italian strong motion data.

The hazard maps have been computed for PGA and Sa(T=1sec) for 475-year return period. To this aim, the numerical computation of Equation (1) was carried out using relatively small increments: 1.0 km for distance, 0.05 for magnitude, and 0.2 for ε. These steps reduce the problems of numerical interpolation commonly used to produce the hazard maps and, from a disaggregation point of view, allow to limit the issues related to the appropriate selection of the bin used to collect the contribution of the hazard variables. In fact, the identification of the modes of the PDFs may depend on the size of the *M*, *R* and ε bins used for disaggregation.

Panel (a) of Figure 2 shows the hazard map for PGA, while panel (b) shows the map for Sa(T=1sec); both are expressed in units of g. Due to the values of the input parameters and its areal extension, the most hazardous seismic zone is the zone 927.

To better understand the results for the region, the hazard computed for two specific sites is discussed. The selected sites, shown in Figure 1, are Sant'Angelo dei Lombardi, indicated as S1 (latitude: 40.8931N, longitude: 15.1784E), and Ponticelli (Naples), indicated as S2 (latitude: 40.8516N, longitude: 14.3446E). The site-specific analysis will be used to show how the hazard at the two sites can be affected by the parameterization of the selected seismogenic zones. The UHSs are also used to be compared to that provided by INGV, which may be considered as a benchmark. The comparison is only qualitative because INGV used a more sophisticated approach, based on logic tree accounting for several attenuation relationships, a larger number of seismic zones and parameters

(e.g., *b*-values, activity rates, maximum magnitude, etc.) that refer to both statistical and historical completeness of the earthquake catalogue.

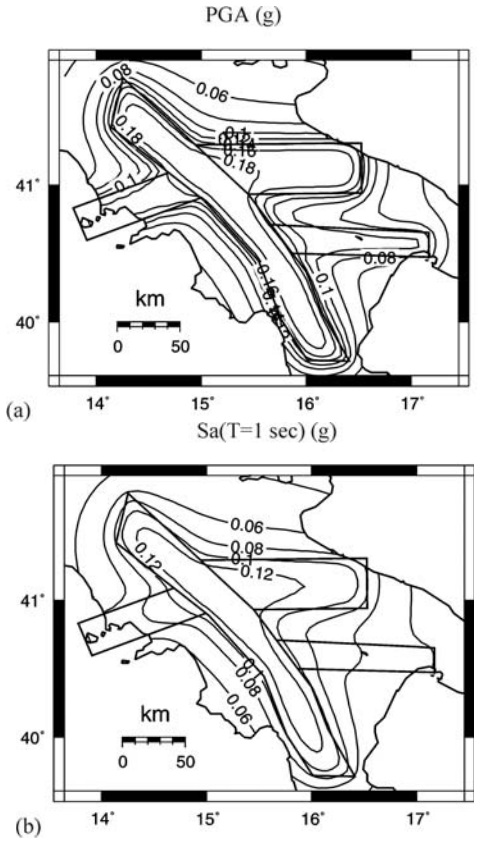

Figure 2: Hazard maps for PGA (a) and Sa(T=1sec) (b) expressed in units of g for a 475-year return period.

In Figure 3 the UHSs, corresponding to 475-year return period, calculated at 11 structural periods, for the two sites are shown. In the same figure the UHSs, retrieved from the INGV website, are also shown. The two UHSs from the INGV website correspond to the closest grid point from the two sites S1 and S2 selected for the present study. Note that the UHSs are comparable, indicating general consistency between the hazard computed in the present study and that by INGV. For the selected sites, the disaggregation analysis was also compared to that of INGV, which, through the http://esse1.mi.ingv.it/ website, provides disaggregation of seismic hazard in form of contribution of bins of M and R. In particular, a bin of 0.5 is used for M while a bin of 10 km is used for R. Concerning the ε variable, only the mean value from disaggregation is provided. The comparison of disaggregated values in terms of modal and mean values for the two sites, obtained from the joint PDFs, for PGA is listed in Table 2.

In particular, ($\overline{M}, \overline{R}, \overline{\varepsilon}$) refers to the mean values while (M^*, R^*, ε^*) refers to the modal values. The results confirm also that, in terms of disaggregation, the present study and that of INGV are in general agreement. Table 3 lists the modal and mean values for the hazard variables for the two selected sites for Sa(T=1sec).

Table 2: Modal and mean values for the hazard variables for the two selected sites S1 and S2 and for PGA. The values have been retrieved from the joint PDFs. ($\overline{M}, \overline{R}, \overline{\varepsilon}$) refer to the mean values while (M*, R*, ε*) refers to the modal values. NA refers to values not available.

S1	*Sant'Angelo dei Lombardi*		
	M^*	R^* (km)	ε^*
INGV	5.5-6.0	0.0-10.0	NA
This study	5.4	4.50	0.4
	$\overline{M}$	$\overline{R}$ (km)	$\overline{\varepsilon}$
INGV	6.06	8.44	0.76
This study	6.02	9.29	0.47
S2	*Ponticelli*		
	M^*	R^* (km)	ε^*
INGV (First mode)	4.5-5.0	0.0-10.0	NA
Second Mode	7.0-7.5	50.0-60.0	NA
This study (FirstMode)	5.50	5.50	0.4
Second Mode	7.0	41.50	1.4
	$\overline{M}$	$\overline{R}$ (km)	$\overline{\varepsilon}$
INGV (First mode)	5.05	9.91	1.00
Second Mode	-	-	-
This study (FirstMode)	5.21	6.09	0.67
Second Mode	-	-	-

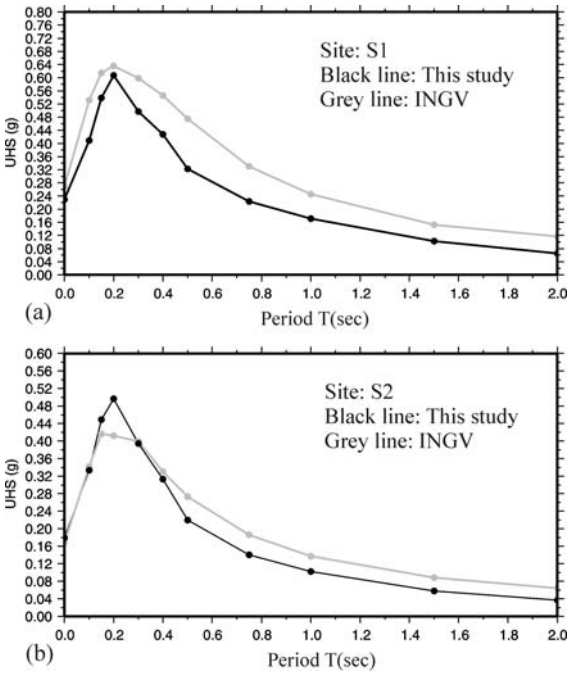

Figure 3: Panel a: uniform hazard spectrum in g for site S1, panel b for site S2 for the return period TR= 475 years. Grey lines refer to the results provided by INGV and black lines refer to the results obtained in this study.

Table 3: Modal and mean values for the hazard variables for the two selected sites S1 and S2 and for Sa(T=1sec). The values have been retrieved from the joint PDFs. ($\overline{M}, \overline{R}, \overline{\varepsilon}$) refers to the mean values while (M*, R*, ε*) refers to the modal values.

S1	Sant'Angelo dei Lombardi					
	M^*	R^* (km)	ε^*	$\overline{M}$	$\overline{R}$ (km)	$\overline{\varepsilon}$
This study	6.2	8.5	0.4	6.34	16.11	0.504
S2	Ponticelli					
	M^*	R^* (km)	ε^*	$\overline{M}$	$\overline{R}$ (km)	$\overline{\varepsilon}$
This study (First Mode)	5.3	4.50	0.4	5.861	25.83	0.712
Second Mode	7.0	66.50	0.4	-	-	-

Figures 4 and 5 show the results of the disaggregation for the sites S1 and S2 respectively, obtained in the present study in terms of both joint and marginal PDFs. Because the joint PDF of Equation (3) may not be represented in a figure, the three bivariate PDFs shown have been obtained by marginalizing each time on the third hazard variable not given in the plot.

As an example, Equation (4) indicates how to obtain the joint PDF of M and R only from that of M, R and ε.

$$f(m,r|A>A_o)=\int_{\varepsilon} f(m,r,\varepsilon|A>A_o)d\varepsilon \qquad (4)$$

In each figure, left and right panels give the contributions, in percents, to PGA and Sa(T=1sec) hazards, respectively. The central part of each panel shows specific joint PDFs for two of the three hazard variables. On the external axes, the marginal PDFs obtained from the joint PDFs are shown. The dashed black lines on the same axes refer to the results provided by INGV for PGA.

As expected, disaggregation shows different results for the two sites. The joint and marginal PDFs for the site S1 have an unimodal shape both for PGA and Sa(T=1sec). This is because the zone 927 (Figure 1), where site S1 is located, represents the most hazardous zone in terms of activity rate and maximum magnitude. On the other hand, the PDFs for the site S2 are characterized by a bimodal shape for both PGA and Sa(T=1sec). In fact, the disaggregated hazard level at site S2 is affected by both the zone 928 where the site is located and the nearest zone 927 (Figure 1). This is confirmed by the presence of a most prominent mode which corresponds to M 5.5 that is very close to the maximum magnitude value selected for zone 928 and a distance of 5.50 km. Although this first mode represents the greatest single contributor to the hazard, it may yet constitute a fraction of the total hazard from all other contributions. In fact, a second mode corresponds to magnitude and distance values that identify another design earthquake located in the zone 927 at a distance of 41.50 km having a M 7.0 that is very close to the maximum magnitude expected for that zone.

As an additional feature, a difference between PGA and Sa(T=1sec) in the hazard contributions of the second mode can be noted. The larger contribution of high magnitude distant events, observed in disaggregation of Sa(T=1sec) hazard with respect to that of PGA, can be ascribed to their lower frequency content compared to lower magnitude nearby earthquakes affecting the spectral ordinates more at high frequency. As a consequence, for the selected spectral ordinate and return period, at least two design earthquakes do exist.

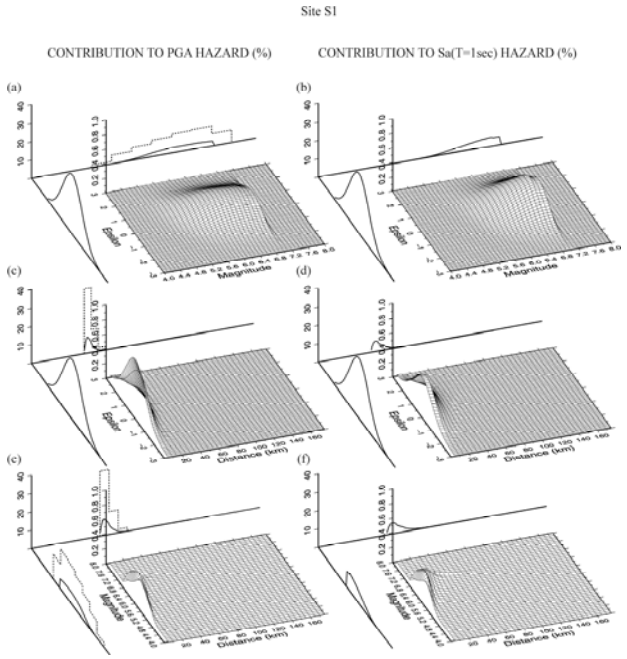

Figure 4: Disaggregation results expressed as contribution to 475-year return period hazard for the site S1. Left panels refer to PGA while right panels refer to Sa(T=1sec).

While the contribution of the second mode to PGA hazard (Figure 5) may be eventually considered negligible, it is significant for Sa(T=1sec), and of engineering interest. Although its contribution does not dominate disaggregation of Sa(T=1sec) hazard because of its lower frequency of occurrence, an engineer should prudently consider it in design as it produces ground motion, having different characteristics with respect to the other design

earthquake, which may affect the construction being designed.

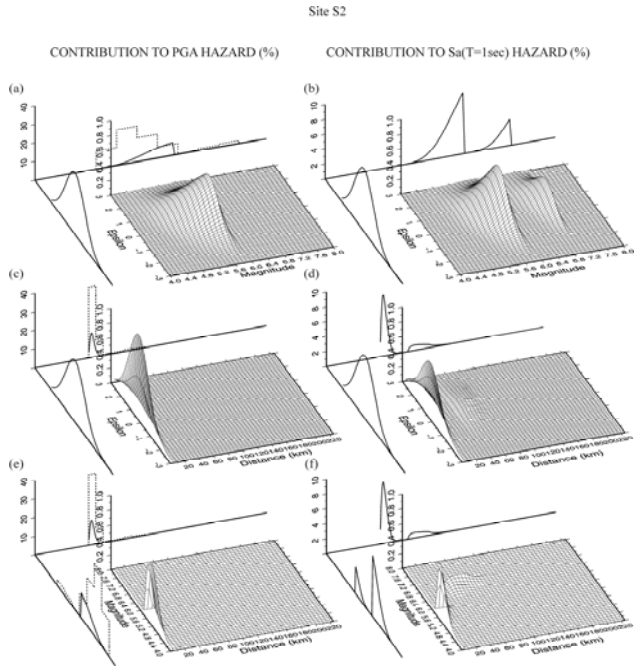

Figure 5: Same as Figure 4 but for site S2.

These results have an important implication for this and other sites in the study region (as shown in the following). Because the fundamental period of most common engineering structures (i.e., buildings) is closer to 1sec than 0sec (corresponding to PGA), and a correlation exists between spectral ordinates at close periods (Inoue and Cornell, 1990), it may be not perfectly appropriate referring to disaggregation of PGA for the identification of the design earthquakes.

In fact, a sound definition of the design earthquakes is important because, engineers who cannot afford to input the hundreds or thousands of earthquake ground motions that are effectively considered in Equation (2) into their analyses, at least need to consider the most relevant for the structural system for which the seismic assessment is carried out. The *M*-*R*-ε maps in the following section help to define those major contributing earthquakes as a function of spectral frequency, hazard level, and location in southern Apennines.

4 MAPS OF THE DESIGN EARTHQUAKES

After computing the 475-year return period hazards for both PGA and Sa(T=1sec), disaggregation was performed. The disaggregated *M*-*R*-ε values were developed for the area shown in Figure 1. Figure 6 shows the design earthquake maps in terms of magnitude, distance and ε for PGA. In particular, left panels refer to the first mode of the joint PDF at each site, while right panels refer to the second mode, if it exists. The latter being identified by imposing that the differences between the relative maxima of the joint PDF were at least 0.25 in units of magnitude or 5.0 km in terms of distance or 0.25 in terms of ε. Figure 7 shows the same results but for Sa(T=1sec) indicating a strong correlation of the identified design earthquakes with the geometry of the seismic zones and both maximum magnitude values and activity rates selected (see Table 1). A single design earthquake cannot be selected for both PGA and Sa(T=1sec) for a large portion of the study area. Larger magnitudes are required to explain target hazard values for Sa(T=1sec) with respect to PGA. Except for the 926 and 928 seismic zones (Figure 1), for the selected return period and particularly for PGA, the identification of hazard-dominant design earthquakes simply looking at the first mode, requires the selection of earthquakes with magnitude around M 6.0 located at distances less than 10 km. Moreover, the magnitudes associated with the first mode correspond to values very close to the maximum magnitude expected for the seismic zones (Table 1). On the other hand, the second mode corresponds to larger magnitude values and larger distances which account for the effect of other zones more hazardous with respect to that where the site is located.

Concerning the disaggregation in terms of distance, the results show a quite regular pattern. The distance associated with the design earthquakes increases as the distance of the site from the seismogenic areas increases. This affects both PGA and Sa(T=1sec) in the 927 and 926 zones, where there is a difference of 3 in unit of magnitude values between first and second mode and at least a variation of 50 km in distance.

Disaggregation on the epsilon variable always shows positive values for all the zones with values ranging between 0.0 and 3.0, and in particular larger values are associated with second modes. This is consistent with the selected return period; in fact, larger ε values are associated to higher hazard levels.

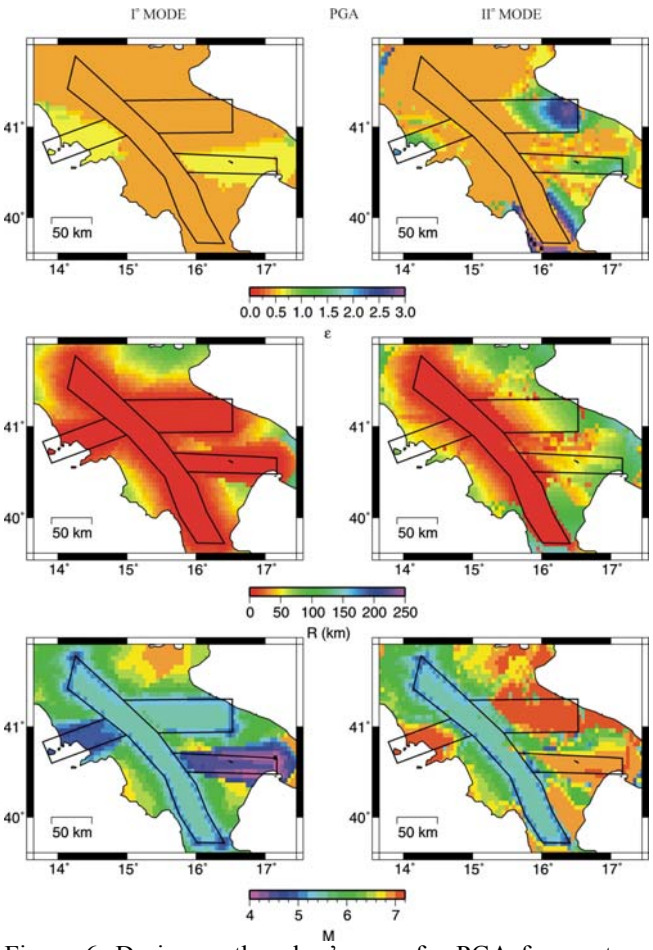

Figure 6: Design earthquakes' maps for PGA for a return period of 475 years. For each hazard variable, left panels refer to the first mode of the joint PDFs while right panels refer to the second mode of the joint PDFs.

To assess how much the two modes contribute to hazard for both PGA and Sa(T=1sec), the differences in contribution to the hazard of the modal values were calculated at each site. This was carried out considering the two modes from the joint PDFs (Figure 6 and 7), but also considering the first two modes identified on the marginal *M*, *R*, and ε PDFs separately. This allows one to assess whether using marginal or joint PDFs from disaggregation leads to different conclusions on the design earthquakes in the study region. Figure 8 shows the results of the analysis for PGA (left panel) and Sa(T=1sec) (right panel). The ΔF index corresponds to the relative contribution to the hazard ($\Delta F=F^{II}/F^{I}$) of the second mode (F^{II}) with respect to the first mode (F^{I}). The white areas indicate sites where PDFs feature a single mode. Joint PDFs show larger areas where a second mode can be identified with respect to the marginal PDFs. For the areas external to the seismic zones, the second mode gives a comparable contribution to the hazard with respect to the first mode. This is because for those sites, multiple zones giving comparable contributions to the hazard exist.

The analysis of ΔF confirms what was observed for site S2 and shown in Figure 5, i.e., the second mode gives a much higher contribution in the case of Sa(T=1sec) with respect to PGA. As expected, there is not a match between the results obtained from the joint and the marginal PDFs for the whole study area.

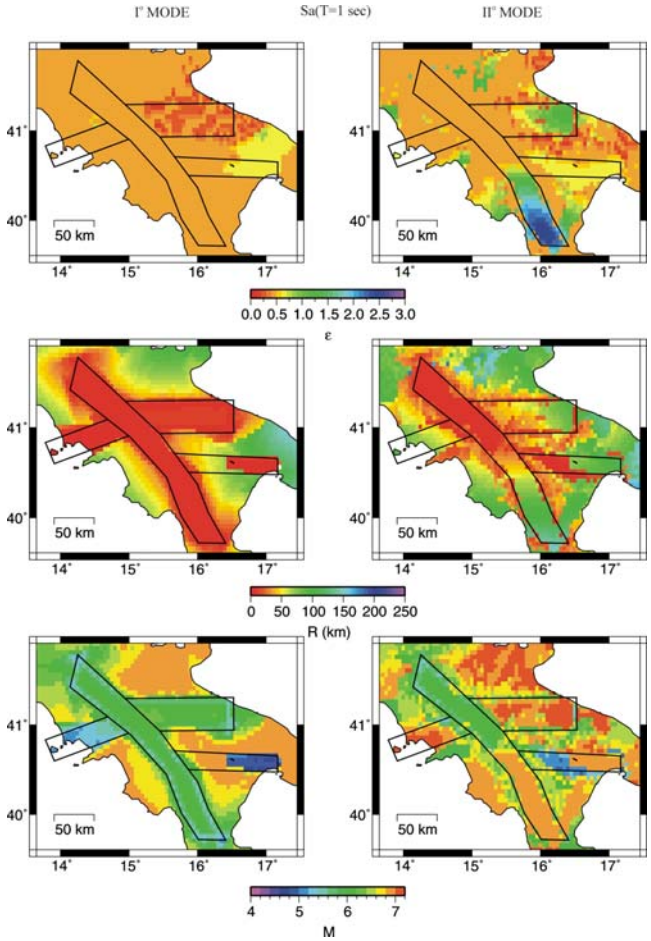

Figure 7: Same as Figure 6 but for Sa(T=1sec).

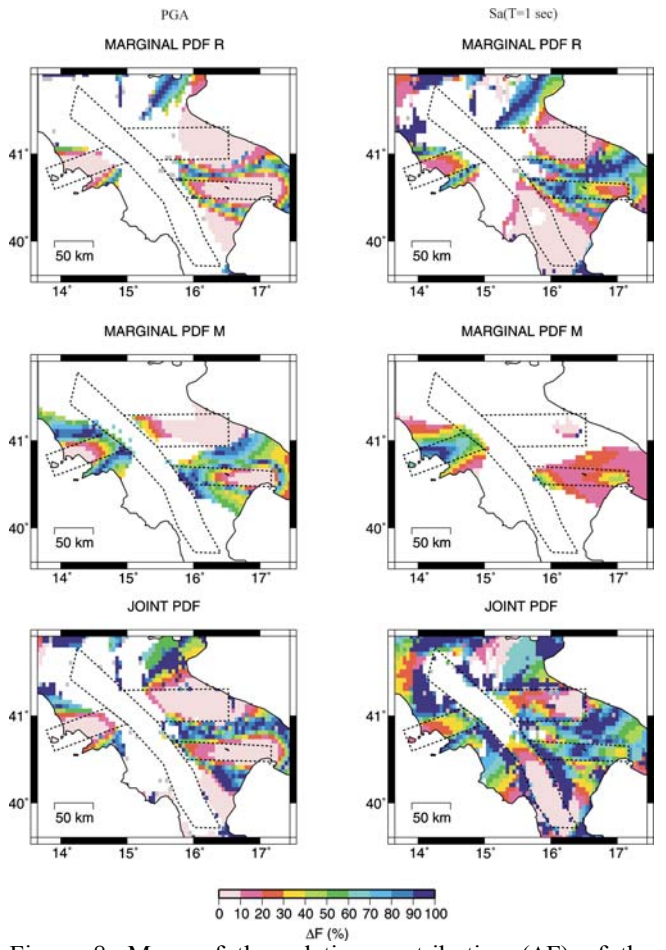

Figure 8: Maps of the relative contribution (ΔF) of the second mode with respect to the first mode of the PDFs obtained from disaggregation analysis. Left panels refer to PGA and right panels refer to Sa(T=1sec).

5 CONCLUSIONS

The problem of selecting the design earthquake in southern Apennines, Italy, for earthquake engineering purposes was investigated using the probabilistic seismic hazard and disaggregation analyses. The design earthquakes for the area of interest were identified and mapped in order to illustrate the correlation with the geometry of the seismogenic zones and earthquake recurrence modelling parameters.

In the first stage of the study, the hazard analysis for PGA and the spectral acceleration at T=1sec, was performed. The acceleration values corresponding to a 475-year return period were mapped. The application considered four seismic zones, which are the same of the national hazard study acknowledged by the Italian seismic code. Subsequently, the corresponding design earthquakes, in terms of magnitude, distance and ε, were mapped. Site-specific analyses and disaggregation maps have shown that for a large part of the study area disaggregated joint and marginal PDFs are characterized by at least a bimodal shape. The contribution to the hazard of the second modes is larger for Sa(T=1sec) than for PGA and depends on the seismogenic zone. The first modes for both spectral ordinates indicate that the magnitude of design earthquake has to be around M 6 for the central part of the southern Apennines. On the other hand, the zones 926 and 928 are characterized by magnitude around M 4.5 and 5.0 respectively. Magnitude values increase for all the seismogenic zones when the second modes are taken into account. The larger increase is in the zone 926 where the values change from M 4.5, for the first mode, to M 7.0 for the second mode. The increase in the magnitude implies an increase of the distances at which the design earthquake has to be located. The analysis of the first mode shows that, for the sites located within the seismogenic areas, the largest contribution to the hazard comes from the inner part of the same zones. On the other hand, the analysis of the second modes shows that there is always a twofold contribution to the hazard that depends on the relative position of the site with respect to seismogenic areas.

Finally, maps of the relative contribution (ΔF) of the second mode with respect to the first mode of the disaggregated marginal and joint PDFs were produced. As it is expected, the pattern of marginal PDFs is not matched by the pattern of the joint PDFs. In fact, the marginalization may lead to modal M, R pairs (i.e., the design earthquakes) different in number, values of the variables, and contribution to the hazard with respect to the joint PDF.

If disaggregation of Sa(T=1sec) hazard is considered, the maps of ΔF show that the PDFs for many sites feature a bimodal shape indicating multiple design earthquakes, which may be significant for engineering purposes. Conversely, disaggregation of PGA hazard is typically unimodal or characterized by a second mode modestly contributing to the hazard with respect to the first mode, which could lead a practitioners to consider only the latter and to imprudently neglect the former.

In conclusion, mapping the design earthquake may prove useful and can be used as additional information with respect to the classic hazard maps. It allows the practitioner to account for the effect of multiple events and ground motion parameters in the selection of proper design earthquakes for engineering risk assessment purposes in those region, as the one the study refers to, where PSHA is based on seismogenic zones.

REFERENCES

Bazzurro, P., and C. A. Cornell (1999). Disaggregation of seismic hazard, *Bulletin of the Seismological Society of America,* **89,** 501-520.

Bommer, J. J. (2004). Earthquake actions in seismic codes: can current approaches meet the needs of PBSD?, in *Performance Based Seismic Design Concepts and Implementation*. PEER Report 2004/05, Pacific Earthquake Engineering Research Center University of California Berkeley, CA.

CEN, European Committee for Standardisation TC250/SC8/ [2003] Eurocode 8: Design Provisions for Earthquake Resistance of Structures, Part 1.1: General rules, seismic actions and rules for buildings, PrEN1998-1.

Convertito, V., and A. Herrero (2004). Influence of focal mechanism in probabilistic seismic hazard analysis, *Bulletin of the Seismological Society of America,* **94**, 2124-2136.

Cornell, C. A. (1968). Engineering seismic risk analysis, *Bulletin of the Seismological Society of America,* **58**, 1583-1606.

Cornell, C. A. (2004). Hazard, ground motions and probabilistic assessment for PBSD, in Performance Based Seismic Design Concepts and Implementation. PEER Report 2004/05, Pacific Earthquake Engineering Research Center University of California Berkeley, CA.

Cramer, H. C., and M. D. Petersen (1996). Predominant seismic source distance and magnitude for Los Angeles, Orange, and Ventura Counties, California, *Bulletin of the Seismological Society of America,***86**, 1645-1649.

Gruppo di lavoro CPTI (2004). Catalogo Parametrico dei Terremoti Italiani, versione 2004 (CPTI04), INGV, Bologna.

Harmsen S. and A. Frankel (2001). Geographic deaggregation of seismic hazard in the United States, *Bulletin of the Seismological Society of America,* **91**, 13-26.

Iervolino, I., and C. A. Cornell (2005). Record selection for nonlinear seismic analysis of structures, *Earthquake Spectra*, 21, 685-713.

Iervolino, I., and C. A. Cornell (2008). Probability of occurrence of velocity pulses in near-source ground motions, *Bulletin of the Seismological Society of America,*. **98**: 2262-2277.

Iervolino, I. G. Maddaloni, and E. Cosenza (2008). Eurocode 8 compliant real record sets for seismic analysis of structures, *Journal of Earthquake Engineering*, **12**(1), 54-90.

Inoue, T., and C. A. Cornell (1990). *Seismic Hazard Analysis of Multi-Degree-of-Freedom Structures*, Reliability of Marine Structures, RMS-8, Stanford, California, 70 pp.

McGuire, R. K. (1995). Probabilistic seismic hazard analysis and design earthquakes: Closing the loop, *Bulletin of the Seismological Society of America,* **85**, 1275-1284.

Meletti, C., and V. Montaldo (2007). Stime di pericolosità sismica per diverse probabilità di superamento in 50 anni: valori di a_g, *Progetto DPC-INGV S1, Deliverable D2*. [http://esse1.mi.ingv.it/d2.html] (in Italian).

Meletti, C., F. Galadini, G. Valensise, M. Stucchi, R. Basili, S. Barba, G. Vannucci, and E. Boschi (2008). A seismic source zone model for the seismic hazard assessment of the Italian territory, *Tectonophysics* **450,** 85–108.

CS.LL.PP, DM 14 gennaio, (2008). Norme Tecniche per le Costruzioni, *Gazzetta Ufficiale della Repubblica Italiana*, 29 (in Italian).

Montaldo, V., and C. Meletti (2007). Valutazione del valore della ordinata spettrale a 1 sec e ad altri periodi di interesse ingegneristico, *Progetto DPC-INGV S1, Deliverable D3*. [http://esse1.mi.ingv.it/d3.html] (in Italian).

Montone, P., M. T. Mariucci, S. Pondrelli, and A. Amato (2004). An improved stress map for Italy and surrounding regions (central Mediterranean), *Journal of Geophysical Research*, **109**, B10410, doi:10.1029/2003JB002703.

Reiter, L., 1990. *Earthquake Hazard Analysis: Issues and Insights*, Columbia University Press.

Sabetta, F., and A. Pugliese (1996). Estimation of response spectra and simulation of non stationary earthquake ground motion, *Bulletin of the Seismological Society of America,* **86**, 337-352.

Spallarossa D., and S. Barani (2007). Disaggregazione della pericolosità sismica in termini di M-R-ε, *Progetto DPC-INGV S1*, *Deliverable D14*. [http://esse1.mi.ingv.it/d14.html] (in Italian).

U.S. Nuclear Regulatory Commission (2001). Technical Basis for Revision of Regulatory Guidance on Design Ground Motions: Hazard- and Risk-Consistent Ground Motion Spectra Guidelines, NUREG/CR-6728, Government Printing Office, Washington, D.C.

Valensise G., A. Amato, P. Montone, and D. Pantosti (2003). Earthquakes in Italy: past, present and future, Episodes, Vol. **26**, 245-249.

Westaway, R., and J. Jackson (1987). The earthquake of 1980 November 23 in Campania-Basilicata (southern Italy), *Geophys. J. R. Astron. Soc.*, **90**, 375-443.